International Journal of Integrated Engineering, Vol. 10 No. 4 (2018) p. 156-164

DOI: https://doi.org/10.30880/ijie.2018.10.04.025

An Analysis of Chemical-Mechanical Damage in Reinforced Concrete Beam

Hamidun Mohd Noh[1,*], Yoshimi Sonoda[2], Hiroki Tamai[3], Isao Kuwahara[4]

[1234]Department of Civil Engineering
Kyushu University, Motooka 744, Nishi-ku, Fukuoka, 〒819-0395, JAPAN.
[1]Department of Construction Management
Faculty of Technology Management and Business, Universiti Tun Hussein Onn Malaysia, 86400 Parit Raja, Johor, MALAYSIA

Abstract: Nowadays, a major issue in the field of construction is the deterioration of reinforced concrete structures due to chemical and mechanical attacks. This deterioration directly impacts construction safety and serviceability, as well as the cost of maintenance. For the purpose of maintaining safety and serviceability, it is necessary to evaluate the durability of existing structures accurately, in order to predict the structure's deterioration and its future strength. In this study, an experiment was conducted in which the electrolytic process was carried out for several levels of corrosion. Next, a static loading test was adopted to assess the structural performance and obtain the ultimate strength of the beam. In addition, continuum damage mechanics were utilized in the analysis of damage caused by chemical and mechanical effects. Within the framework of this method, chemical damage caused by the corrosion of steel bars was considered. Then the coupling effects of chemical and mechanical damage were calculated by introducing two independent scalar damage variables into the constitutive equation. To calculate the chemical damage evolution, we carried out a diffusion process of chloride ions that impact the corrosion of steel bars in concrete, and an evaluation was conducted on an affected cross-sectional area of a steel bar. The proposed method was found to validate the experiment's results and could predict the ultimate strength under various exposure conditions. Moreover, the proposed orthotropic conditions may be carried out as an alternative to isotropic analysis in order to identify the worst-case scenario of the structure.

Keywords: *Corrosion, coupling effects, chloride attack, mechanical damage, orthotropic, isotropic, diffusion*

1.0 Introduction

The deterioration of concrete is a long-term problem occurring around the world, not only in aged structures, but also in newly constructed ones. Environmental factors play a key role in the initiation of corrosion in concrete structures. Once there is sufficient moisture and oxygen in the environment, corrosion begins and these factors control the rate of deterioration.

Generally, the corrosion in concrete can be introduced in a three-stage process. The first stage is initiation, where the diffusion of CO_2 or chloride ions through concrete covers causes depassivation to the steel reinforcement. In the next stage, the steel reinforcement starts to corrode, thereby producing corrosion products and generating expansive pressure on the concrete surface. The final stage involves deterioration processes such as the cracking, spalling and delamination of concrete structures.

There are several factors affecting the durability of concrete structures. The durability of concrete structures is influenced by mix proportion factors such as cement type, concrete cover, casting method, curing process and other execution conditions [1]. Besides these, environmental factors such as the distance from the structure to the sea, climate and temperature, humidity and other geomorphic conditions contribute much to the invasion of chloride ions on concrete surfaces [2]. Moreover, mechanical factors such as excessive loads impacting on the structure also increase the level of deterioration.

Since chloride ion invasion is the most threatening factor, many studies conducted on chloride-induced corrosion involve laboratory studies or accelerated experiments simulating real conditions, and studies are also carried out in real structures. Investigations of durability, followed by predicting the future strength of concrete structures are important issues to highlight in order to improve efficiency in safety, serviceability and performance. In addition, the maintenance costs of the structure can be kept to a minimum.

Therefore, the experiments in this study first considered the degradation process due to mechanical and chemical attacks. Secondly, a numerical model was created to simulate and validate the experimental results. Next, the future strength of the concrete structure in the next 20 and 40 years was predicted. After that, a comparison between isotropic and orthotropic analysis

*Corresponding author: hamidun@doc.kyushu-u.ac.jp / hamidun@uthm.edu.my

condition was carried out. Lastly, the severity of the conditions of RC structures in marine environments was reviewed.

2.0 Damage Assessment of RC Structure

2.1 Overview of Continuum Damage Mechanics

The damage process can be described as an irreversible phenomenon of material deterioration involving the growth of defects and cavities in micro-scale. In continuum damage mechanics, the degree of material degradation in a homogenous field is assumed as the damage variable. Lemaitre and Desmorat [3] interpreted the physical meaning of damage to be the decrease in area for effective load carrying, due to void development as the following:

$$D = \frac{A_D}{A_o} \tag{1}$$

where A_0 is the total area of the cross section and A_D is the area of all defects. Thus, the general constitutive equation can be introduced as:

$$\sigma_{ij} = (1 - D)E_{ijkl}\varepsilon_{kl} \tag{2}$$

where σ_{ij} is the stress tensor, ε_{kl} is the strain tensor, E_{ijkl} is the elastic stiffness tensor and D is the damage variable.

In this study, the mechanical damage variable is represented by three different component vectors while the chemical damage is an isotropic scalar variable. It is also assumed that material deterioration caused by the coupling effect between chemical and mechanical damage could be described by the following relationship:

$$\sigma_{ij} = (1 - D_{mech})(1 - D_{chem})E_{ijkl}\varepsilon_{kl} \tag{3}$$

where D_{mech} is the mechanical damage variable and D_{chem} is the chemical damage variable.

2.2 Mechanical Damage Model

Fig. 1 shows the material properties of the concrete and steel reinforcement bars used in the numerical analysis. For the rebar, assumed to have a complete elasto-plastic body, we adopted the constitutive law based on the von Mises yield condition. As for the concrete, we applied the elastic-plastic constitutive law based on the Drucker-Prager yield condition.

The rate of degradation due to corrosion is defined by the degree of damage in three principal axis directions as $\emptyset_x, \emptyset_y$ and $\emptyset_z$ assuming the tension to be softening. In order to adequately assess the progress of cracks in the concrete, it is necessary to release the tension softening stress by the subsequent tensile strength. After that, only the extracted positive principal strain components (the degree of damage in principal strain directions D_x^L, D_y^L and D_z^L) are converted to the whole coordinate axes of D_x^G, D_y^G and D_z^G. The rate of degradation for each coordinate axis direction was calculated by the following Equations (4) to (6).

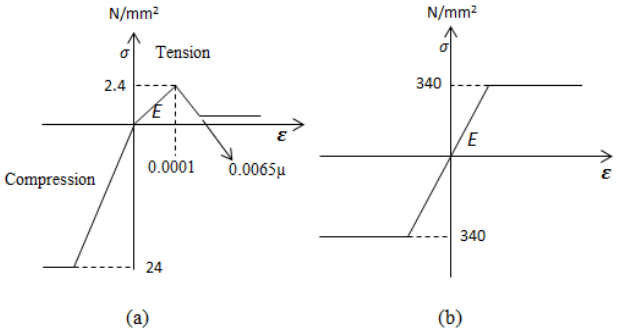

Fig. 1 Material properties of (a) concrete and (b) steel bar.

$$\emptyset_x = \sqrt{1 - D_x^G}, \left(D_x^L = \frac{\varepsilon_x^L}{\varepsilon_u} \right) \tag{4}$$

$$\emptyset_y = \sqrt{1 - D_y^G}, \left(D_y^L = \frac{\varepsilon_y^L}{\varepsilon_u} \right) \tag{5}$$

$$\emptyset_z = \sqrt{1 - D_z^G}, \left(D_z^L = \frac{\varepsilon_z^L}{\varepsilon_u} \right) \tag{6}$$

Equations (4) to (6) demonstrate the relationship between $\emptyset_x, \emptyset_y$, $\emptyset_z$ and D_x^G, D_y^G and D_z^G with the definition of D_x^L, D_y^L, D_z^L. Here, ε_u is defined as the tensile strain limit. In addition, the relationship between the stress rate and the degradation rate associated with the tension softening is defined in Equation (7).

$$\alpha_{xx} = \phi^2_{x,} \quad \alpha_{yy} = \phi^2_{y,} \quad \alpha_{zz} = \phi^2_{z} \tag{7}$$

Furthermore, in this analysis the degradation rate was multiplied by the elastic stiffness matrix. As shown in Equation (8), an isotropic constitutive law with damage influence is obtained.

$$\{\sigma_{ij}\} = \{[D^e] - [D^p]\}\{\boldsymbol{\varepsilon}_{kl}\}$$

$$[D^e] = \begin{bmatrix} \phi_x^2(\lambda+2\mu) & \phi_x\phi_y\lambda & \phi_x\phi_z\lambda & 0 & 0 & 0 \\ \phi_y\phi_x\lambda & \phi_y^2(\lambda+2\mu) & \phi_y\phi_z\lambda & 0 & 0 & 0 \\ \phi_z\phi_x\lambda & \phi_z\phi_y\lambda & \phi_z^2(\lambda+2\mu) & 0 & 0 & 0 \\ 0 & 0 & 0 & \phi_x\phi_y 2\mu & 0 & 0 \\ 0 & 0 & 0 & 0 & \phi_y\phi_z 2\mu & 0 \\ 0 & 0 & 0 & 0 & 0 & \phi_z\phi_x 2\mu \end{bmatrix} \tag{8}$$

2.3 Chemical Damage Model

2.3.1 Chemical Damage Variables

In order to assess the damage caused by the penetration of chloride ions in concrete structures, a diffusion process is carried out. By using a three-dimensional diffusion equation that follows Fick's second law (as shown in Eq. 9), the concentration and distribution of chloride ions along the structure can be determined. Hypothetically, the concentration of chloride ions has a great influence on the level of corrosion of steel bars in RC beams.

$$\frac{\partial C}{\partial t} = K\left(\frac{\partial^2 C}{\partial x^2} + \frac{\partial^2 C}{\partial y^2} + \frac{\partial^2 C}{\partial z^2}\right) \quad (9)$$

where K is the diffusion coefficient and C is the chloride concentration.

In this analysis, the threshold of chloride concentration is set at a value of C=1.2kg/m^3. Therefore, chemical damage is assumed to occur once the threshold value at the interface between the concrete and steel bars is surpassed. As proposed by Sonoda [4], the reduction of the steel bar cross section area is obtained by the following relationship:

$$\omega = 0.02(0.33C_s + 3.7) \quad (10)$$

where ω is the reduction of the steel bar cross section area and C_s is the cumulative chloride concentration at the interface (kg/m^3.year).

In this analysis, the chemical damage variable is referred to as the reduction of the steel bar cross sectional area:

$$D_{chem} = \omega \quad (11)$$

2.3.2 Expansion Pressure Due to Corrosion

Since corrosion is a continuous process, once it is initiated at the surface of the bar-concrete area, the corrosion product grows gradually. Andrade *et al.* [5] proposed a linear relationship between applied current density, I_{corr} and the decreased rebar diameter based on Faraday's law:

$$2R_{rb} = 2R_b - 0.023\, i_{corr}\, \Delta t \text{ (mm)} \quad (12)$$

where R_{rb} (mm) is the reduced rebar radius, R_b (mm) is initial rebar radius, I_{corr} is the applied current density (μA/cm^2), 0.023 is conversion factor (from μA/cm^2 to mm per year) and Δt is time since the propagation period (years).

The total radius of the rebar, including the rust layer as illustrated in Fig. 2, can be calculated as:

$$R_r = R_{rb} + t_r \quad (13)$$

where t_r is the thickness of the oxide layer that builds up around the bar. Since β is the relative ratio of steel density to corrosion product density (normally ranging from 2.2 to 6.4 as stated in the literature), the most common value of 2.0 has been used in our analysis [6]. As proposed by Kim *et al*. [8], the expansive pressure induced by the restraint conditions of the surrounding concrete can be calculated by Eq 14:

$$P = K_{rust.}\left[\sqrt{1 + \frac{\left(\frac{R_b}{2} + (R_r - R_{rb}).2\right)^2}{2R_b^2}(\beta - 1)} - 1\right]^m \quad (14)$$

where K_{rust} is the stiffness of the corrosion product layer and m is an empirical constant. In previous research, Lundgren [9] suggested the m value as 7 and the basic image of expansive pressure was illustrated in Fig. 3.

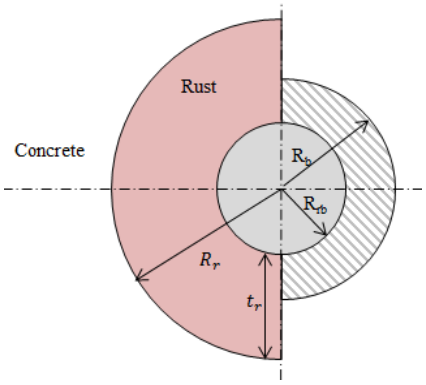

Fig. 2 Rust expansion under concrete constraints.

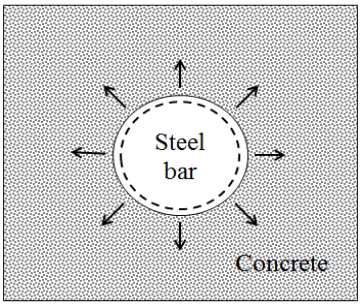

Fig. 3 Graphical image of expansive pressure.

A wide range values expressing the stiffness of the corrosion product or the oxide of Young's moduli can be found in the literature. Molina *et al*. [6] claimed that the values ranged between 2 and 4 GPa while Lundgren [8] proposed a nonlinear stress level independent of the stiffness of the corrosion products, with a maximum value of 14 GPa. On the other hand, Balafas and Burgoyne [9] reported values as low as 40-87 MPa, and as values as high as 47-86 GPa were recorded by Zhao *et al*. [10]. In addition, Savija *et al*. [11] found that the Young's modulus of the rust layer is not constant, as it depends on the level of confinement provided by the surrounding material. However, for simplicity, Lungren [8] proposed a constant value of 7 GPa and this is the

value used in the current study. The expansive pressure calculated in this study is in line with the curve plotted by Lundgren [8] as shown in Fig. 4.

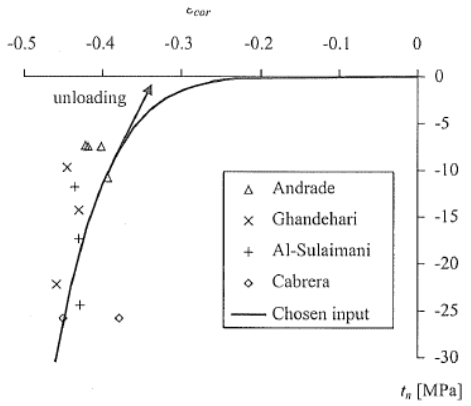

Fig. 4 Normal stress versus strain in the rust evaluated from a combination of experimental results and analysis [8].

3.0 The Experimental Process

3.1 The Electrolytic Corrosion Method

In order to construct the damaged RC beams with corroded reinforcement, the electrolytic corrosion method was chosen. This is one method to accelerate the corrosion of reinforced steel. In this test, a copper sheet reacting as a cathode was linked to the DC power supply generator. As illustrated in Fig. 5, the cathode and specimen were soaked in a 3% NaCl solution. The corrosion level of the steel reinforcement is controlled by the energization time.

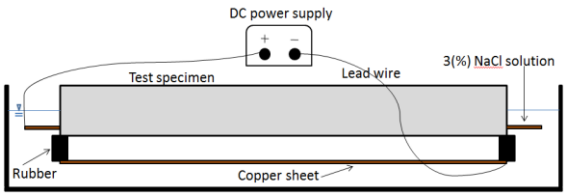

Fig. 5 Set up of the electrolytic corrosion method apparatus.

Once the electrolytic corrosion method test was performed, a loading test was conducted. After that, the steel reinforcements were taken out of the specimen and the corrosion rate was measured and calculated according to the following equation:

$$C = \frac{w_0 - w_{corr}}{w_0} \text{ x } 100 \qquad (15)$$

where C is the corrosion rate, w_0 is the initial mass of the steel reinforcement without corrosion and w_{corr} is the mass of the corroded reinforcement.

3.2 The Electrolytic Corrosion Method

A static loading test was performed to clarify the static flexural load-bearing capacity of RC beams with corroded reinforcements. A universal testing machine was used to put a compressive load on the beams. As shown in Fig. 6 below, at two points a concentrated load of equally bending movement sections of 200 mm was applied at a loading rate of 0.5 mm/min. The displacement meter and the acting load were set up at the mid-span of the beam to measure the displacement and the load acting on the beam.

4.0 The Results of The Experiment

4.1 The Results of The Electrolytic Corrosion Process

After the loading test, three corrosion levels were determined and measured from the electrolytic corrosion process. There was one model with no corrosion and two models with corrosion which was measured at 6.13% and 11.71%, respectively. The crack conditions on the specimen's surface is shown in Fig. 7. This experiment proved that once corrosion is initiated at the steel bar, it will reduce the effective surface of the initial steel diameter. Since corrosion products occupy a larger volume than concrete, their expansion in volume generates tensile stress, which initiates cracks at the concrete surface.

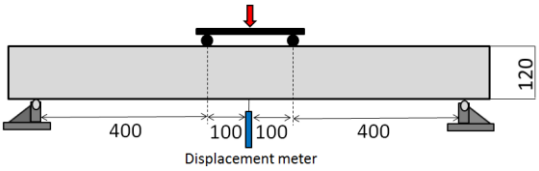

Fig. 6 Details of the position of experimental equipment.

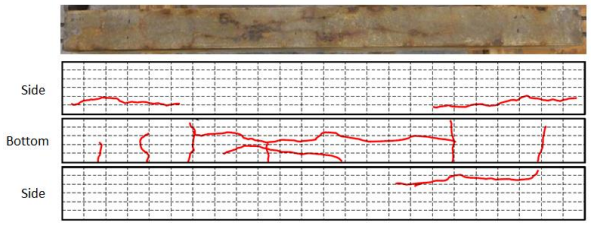

(a) 6.13%

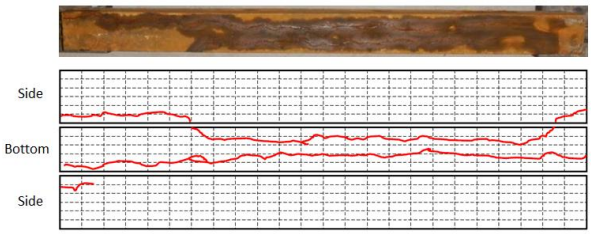

(b) 11.71%

Fig. 7 Crack conditions of RC beam specimens.

4.2 The Results of The Static Loading Test

In order to assess the strength performance of beams after corrosion, a static loading test was carried out and the ultimate strength was obtained. Fig. 8 presents the relationship between the load -bearing capacity and the displacement for different corrosion levels. As can be seen, beams with no damage (without corrosion) reach a maximum strength of 25.72 kN compared to the damaged beams, which expressed values of 22.11 kN and 22.6 kN for 6.13% and 11.71% degrees of corrosion, respectively. This result could be due to the existence of initial cracks caused by corrosion.

Hypothetically, the maximum load-bearing capacity decreases linearly as the degree of corrosion increases. However, the maximum load -bearing capacity for the bar at 11.71% of corrosion exceeded the value for 6.13% corrosion. This is because the increase of density in the beam with the higher corrosion rate, placed between the rebar and the surrounding concrete whose reinforcement expansion was caused by corrosion, dominates the cross-sectional reduction of the effective area for the 6.13% corrosion level. This is why models with lower corrosion levels deteriorate earlier than those with higher corrosion levels.

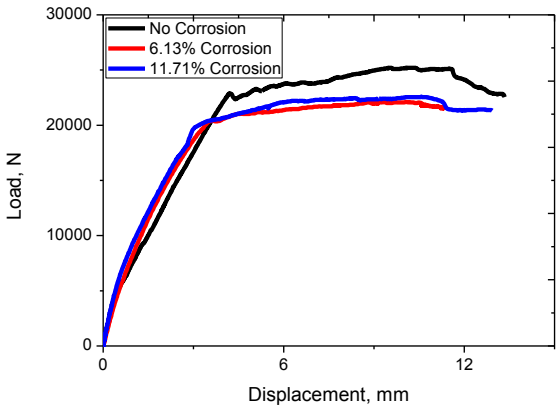

Fig. 8 Load-displacement relationship at different corrosion levels.

5.0 Chemical-Mechanical Damage Analysis

In the previous chapter, an experiment was conducted and the electrolytic process was carried out to corrode the steel reinforcement for several degrees of corrosion. Next, beams were loaded with an external load and the results were obtained. In this chapter, a numerical model was developed to determine the accuracy and thus validate the experiment's results. To perform an assessment of damage caused by chemical-mechanical loading factors, a diffusion analysis and mechanical loading were implemented in the numerical model.

5.1 The Development of The Numerical Analysis Model

In order to validate the experiment's results and to further predict the structural performance of RC structures through several degrees of corrosion and periods of exposure, a three-dimensional finite element model was adopted using the nonlinear finite element code of MARC 2010. Fig. 9 below illustrates the cross-section and the elements of the RC beam consisting of 8 nodes of hexahedral concrete element and reinforcement bars. The concrete and reinforcement bars were classified as solid while the shear reinforcement bar was designed using a (axial) truss element.

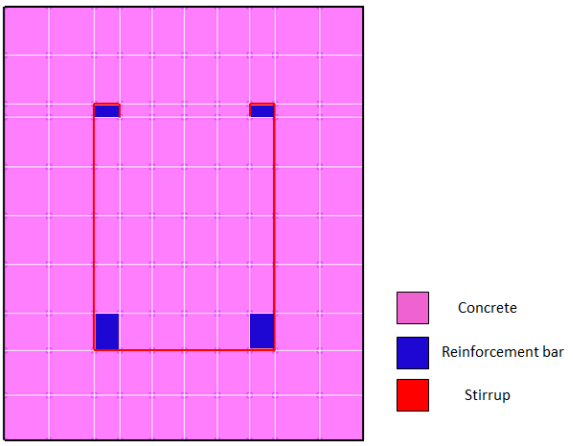

Fig. 9 Cross-section of a beam.

5.2 Validation of Numerical Analysis Accuracy

During the experiment, the cases of three cases of beams were studied. There was a beam with no corrosion and two beams with corrosion initiated at the surface of steel reinforcement set at the corrosion levels of 6.13% and 11.71%. The corrosion of the steel reinforcement bars was initiated by the electrolytic process.

In this numerical model, the effect of corrosion on the steel reinforcement bar was taken into account. The reduction of the initial diameter, the effective area of the rebar and the initiation of expansive pressure from the steel to the concrete surface were calculated then implemented in the numerical analysis model. The results obtained from the experiments are shown and compared with the numerical analysis in Fig. 10. The numerical analysis calculated the behavior of the reinforcement concrete to be similar to the experiments conducted in the laboratory. The analysis started with the linear increment between the load and the displacement at an early stage, then the plot increased gradually to the ultimate strength of the beam when the yield point was surpassed. After reaching the maximum bending capacity, the structure came off as the corrosion created severe conditions since the stiffness decreased due to corrosion, causing noticeable reduction in strength.

It is apparent from the figure that the results from the numerical analysis agree with the experiment's results. The numerical analysis results predicted a higher level of strength for the beam in every case, but this is because perfect bonding and supports between each element were calculated in the analysis. Compare this situation to the experiment, in which bonding and support conditions were not guaranteed to be as perfect as those postulated in

the numerical analysis since there were many uncertainties to be considered.

6.0 Prediction of Future Strength

6.1 Isotropic Conditions

After validating and determining the accuracy of the numerical model, the future strength of concrete beam was predicted. A diffusion analysis was adopted to predict the concentration of chloride ions in concrete and the chemical damage, D_{chem}, caused by chloride invasion to the original beam (shown in Fig. 11(a) was analyzed. A three-dimensional chloride diffusion process in isotropic condition was solved by using the model shown in Fig. 11 (b). The initial condition of chloride concentration and other boundary conditions are assumed as the values in Table 1.

The distribution of chloride ions was obtained from diffusion analysis and Fig. 12 shows the results for different periods of exposure. The influence of chloride ion distribution is directly proportional to increasing service periods whereby the chloride ion reaches the highest concentration at the 40-year period with 2.0 kg/m^3. For the 0-year period, the chloride ions started to penetrate the concrete cover, but the corrosion had not yet initiated, as the chloride ion concentration reached at the surface of steel reinforcements was below the threshold limit. Chemical damage occurred at the exposure period of 20 years, when chloride concentration at the surface of steel bars surpassed the threshold value, 1.2kg/m^3.

When a rebar starts to corrode (axisymmetric corrosion is assumed), a gradual decrease of its diameter is produced, together with the generation of rust. The formation of corrosion products from steel reinforcement bars leads to an increase in volume, generating expansive pressure to the concrete surface. Since corrosion is a continuous process, this expansive pressure keeps increasing between service periods. This pressure may induce the formation of cracks once the concrete's tensile strength is surpassed. The cracks are generated first at the bar-concrete interface, then they propagate radially.

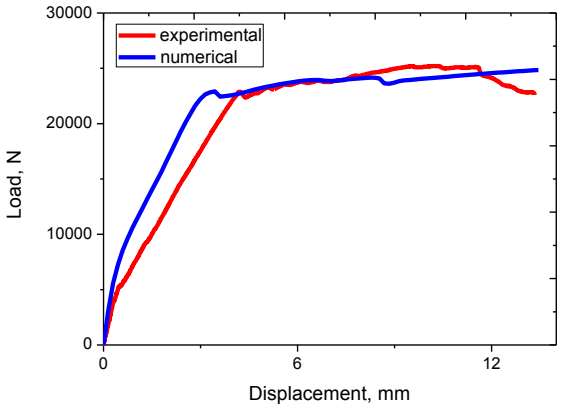

(a) 0% level of corrosion

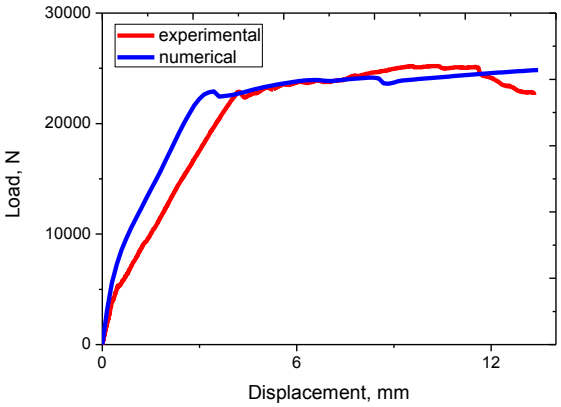

(b) 6.13% level of corrosion

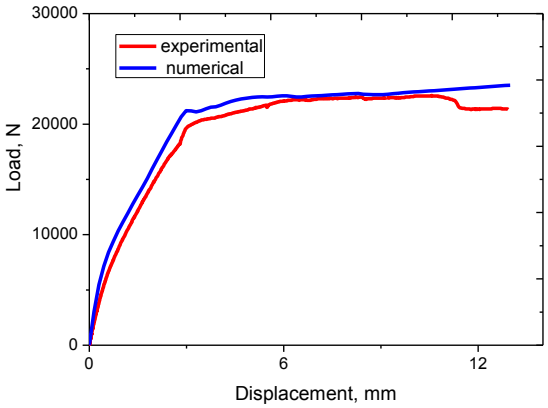

(c) 11.71% level of corrosion

Fig. 10 Numerical-experimental validation for several degrees of corrosion.

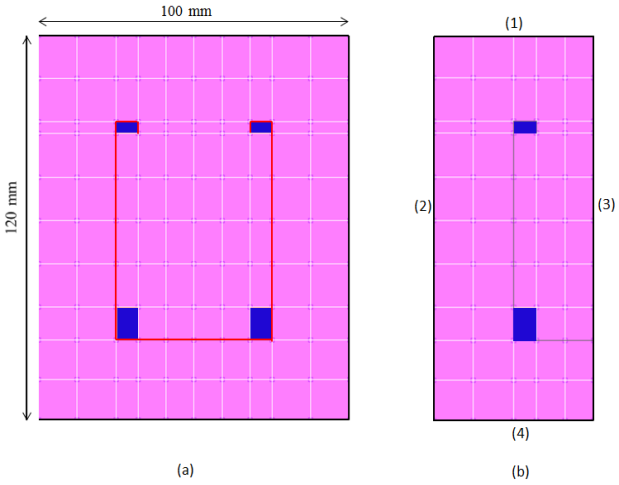

Fig. 11 (a) Original cross-section of the beam (b) Half model used in diffusion analysis.

Table 1 Boundary conditions and material properties for diffusion analysis.

	Isotropic
Cement	Portland cement
Water-cement ratio	45%
Diffusion Coefficient, *K*	1.01 (cm^2/year)
Environmental condition	Splash zone
Initial Chloride concentration	0.0 (kg/m^3)
Chloride concentration of boundary face [(1), (2), (3)]	0.0 (kg/m^3)
Chloride concentration of boundary face (4)	13.0 (kg/m^3)

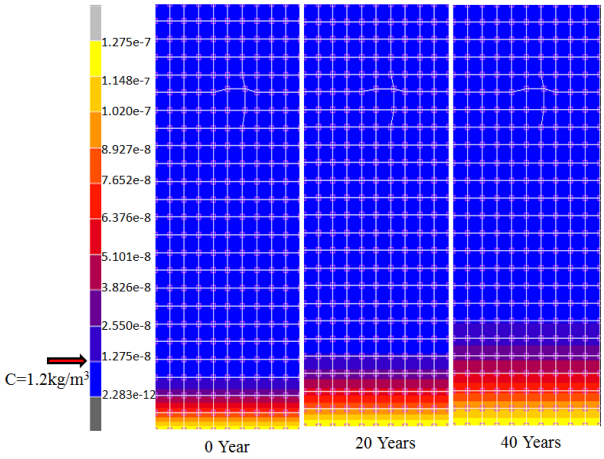

Fig. 12 Chloride concentration distribution of RC beams for different periods of exposure.

Table 2 presents the effects of chloride invasion for different exposure periods. The stress level and the degree of corrosion increased over the years. In the 0-year model, no corrosion was initiated and no expansive pressure was produced. Meanwhile, the value of the chemical damage variable, D_{chem} was 0.082, producing an expansive pressure of about 0.23Mpa. The value of D_{chem} and the expansive pressure then increased for the next 20 years at 0.087 and 0.34Mpa, respectively. This increase in expansive pressure weakens concrete surfaces and generates the formation of cracks. The propagation of cracks and the increase of D_{chem} values reduce the stiffness of the structure and its serviceability, gradually starting the deterioration process.

The last stage in this coupling analysis of chemical-mechanical damage was determining the ultimate strength of RC beams. By applying an external load to the structure model, the mechanical damage variable D_{mech}, was calculated and the load-displacement curve in Fig. 13 was obtained to depict the trend of ultimate strength in different exposure periods. It is clear that the ultimate strength of RC beams decreased with increasing service periods. The period of 0 years of service had the highest load bearing capacity while the 40-year service period had the lowest level of strength.

Table 2 Effects of chloride invasion for each exposure period.

Exposition Year	Chloride Content (kg/m^3)	ω	Expansive Pressure (MPa)
0	-	-	-
20	1.2	0.082	0.23
40	2	0.087	0.34

This is because, over time, the structure was exposed to environmental and mechanical attacks which initiated corrosion. Moreover, the propagation of corrosion product reduced the serviceability and ultimate strength of structure. For these reasons, the exposure periods of a structure have a great influence on the ultimate strength of the RC structure. This condition reviewed the concept of continuum damage mechanics as stated in Equation 3. Since the value of D_{chem} and D_{mech} increases, the material stiffness decreases, directly affecting the reduction of the structure's strength.

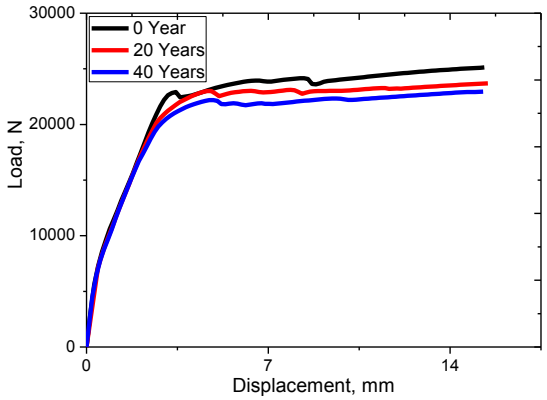

Fig. 13 The ultimate strength of RC beams for different exposure periods.

6.2 Orthotropic Conditions

In contrast to diffusion analysis, orthotropic conditions were carried out by considering the different diffusion coefficient in each axis. The boundary condition and the material properties for the orthotropic analysis are summarized in Table 3. This analysis considered an exposure period of 20 years.

Compared to the previous condition of diffusion analysis, under orthotropic conditions, chloride ions vigorously penetrated the concrete structure, as shown in Fig. 14. With 20 years of exposure, the concentration of chloride ions reaching the surface of the steel bar was 8.73kg/m^3, an increase of about seven times from the previous (isotropic) condition (Table 4).

Since there was a great difference in the distribution of chloride ions penetrating the concrete covers between isotropic and orthotropic conditions, there was a noticeable effect in the relationship of ultimate strength between these two. As shown in Fig. 15, an apparent reduction in the ultimate strength for the orthotropic condition was predicted because it considered

the non-uniform distribution of diffusion exposure whilst the isotropic assumed a uniform condition. This is why considering orthotropic conditions in the analysis of predicting structural strength performance could be taken into account during the design phase as a possible safety precaution.

Table 3 Boundary conditions and material properties for diffusion analysis.

	Orthotropic
Cement	Portland cement
Water-cement ratio	45%
Diffusion coefficient, *K*	Ka = 0.1498 cm^2/year Kb = 2.350 cm^2/year Kc = 0.5 cm^2/year
Environmental condition	Splash zone
Initial Chloride concentration	0.0 (kg/m^3)
Chloride concentration of boundary face [(1), (2), (3)]	0.0 (kg/m^3)
Chloride concentration of boundary face (4)	13.0 (kg/m^3)

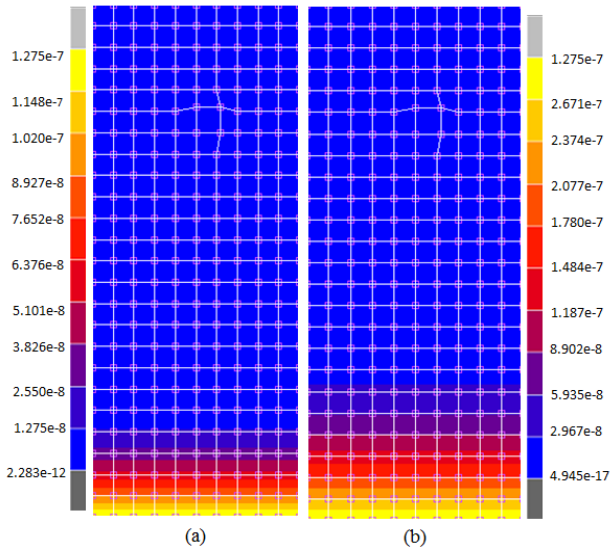

Fig. 14 Comparison of chloride ion distribution between (a) isotropic and (b) orthotropic conditions.

Table 4 Effect of chloride invasion for each analysis condition.

Analysis Condition	Chloride Content (kg/m^3)	ω	Expansive Pressure (MPa)
Orthotropic	8.73	0.132	5.87
Isotropic	1.2	0.082	0.23

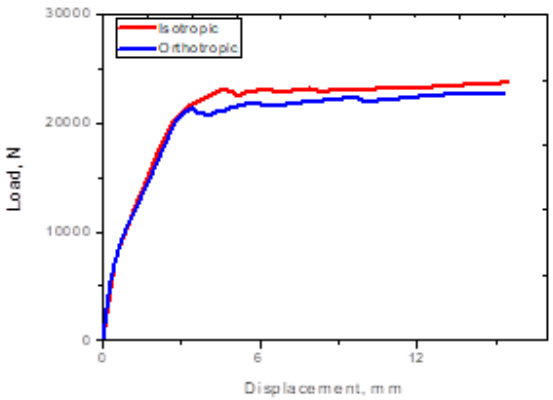

Fig. 15 Load-displacement relationship between isotropic and orthotropic conditions.

6.3 The Influence of Marine Environment on Structural Performance

One important factor in assessing the structural performance of a structure is the environment. In this section, several different environments and conditions were highlighted. In order to understand their impact, two different environments and conditions were compared. For the marine environment, a diffusion coefficient of 4.35cm^2/year was chosen to represent the environment of a coastal area while a diffusion coefficient of 1.44 cm^2/year was used for an inland structural environment [12]. Both cases were considered under both isotropic and orthotropic conditions.

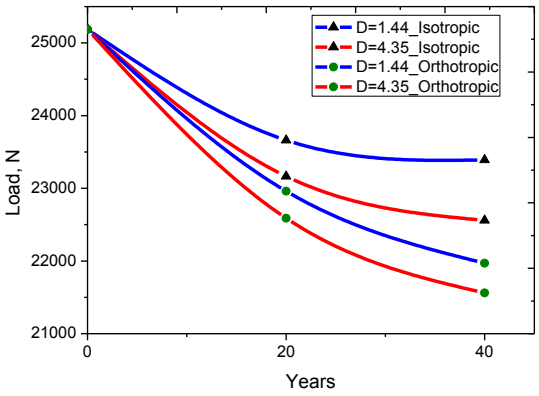

Fig. 16 The ultimate strength for several diffusion coefficients.

In Fig. 16, the ultimate strength for several diffusion coefficients is presented for several periods of exposure. It clearly shows that the increase of diffusion coefficients contributed to the reduction of ultimate strength. These linear relationships continue along with the increase in years of exposure. This is because a larger diffusion coefficient generates a higher chloride ion concentration, directly affecting the increase of D_{chem} values in calculating the coupling effect between chemical and mechanical damage. In the case of coastal areas with high diffusion rates, severe conditions were observed as material stiffness decreased.

7.0 Conclusion

In conclusion, the proposed chemical and mechanical damage analysis tended to validate the results of the experiment. Besides this, we were also able to make predictions of future structural strength under various exposure conditions. In addition, the proposed orthotropic analysis proposed can serve as an alternative to the isotropic conditions in order to identify the worst-case scenario of the structure.

References

[1] Tsutsumi T., Shirai S., Yasuda N. and Matsushima M. Evaluation of parameters effecting chloride induced deterioration based on actual data in situ, *Concrete library of JSCE*, No 30, (1997), pp. 33-41.
[2] Al-Rabiah A.R., Rasheeduzzafar and Baggot R. Durability Requirements for reinforced concrete construction in aggressive marine environments, *Marine Structures* 3, (1990), pp. 285-300.
[3] Lemaitre J. and Desmorat R. (2001). Engineering damage mechanics: ductile, creep, fatigue and brittle failures, *Springer*.
[4] Sonoda Y., Murato N. and Hikosaka H. A fundamental study on deterioration of the existing RC beam by chemical and mechanical damage, *Transaction on Engineering Sciences*, Volume 40, (2003), pp. 295-306
[5] Andrade C., Alonso C., Molina F.J. Cover cracking as a function of rebar corrosion: part I-experimental test, *Mater. Struct. Journal* 26, (1993), pp. 453-464.
[6] Molina F.J., Alonso C. and Andrade C. Cover cracking as a function of rebar corrosion: Part 2 – numerical model. *Materials and Structures*, Volume 29 (9), (1993), pp 532-548.
[7] Kim K.H., Jang S.Y., Jang B.S., and Oh B.H. Modeling mechanical behavior of reinforced concrete due to corrosion of steel bar, *ACI Material Journal*, Volume 107 (14), (2010), pp.106-113.
[8] Lundgren K. Modelling bond between corroded reinforcement and concrete, *Fracture Mechanics and Concrete Structures*, (2001), pp. 247-254.
[9] Balafas I. and Burgoyne C.J. Modeling the structural effects of rust in concrete cover, *Journal of Engineering Mechanics* , Volume 137 (3), (2010), pp. 175-185.
[10] Zhao Y., Dai H. and Jin W. A study of the elastic moduli of corrosion products using nano-indentation techniques, *Corrosion Science*, Volume 65, (2012), pp. 163-168.
[11] Savija B. Lukovic M., Pacheco J. and Schlangen E. Corrosion induced cover cracking studied by X-Ray computed tomography, nanoindentation, and energy dispersive X-Ray spectrometry (EDS). *Materials and Structures* , (2014), pp. 1-20.
[12] Mackechnie J.R. Predictions of reinforced concrete durability in the marine environment, *Research Monograph No.1*. (2001).